

## Freezing-rate effects on the physical characteristics of basal ice formed by net adfreezing

BRYN HUBBARD

*Department of Geography, University of Cambridge, Cambridge CB2 3EN, England*

**ABSTRACT.** A number of theoretical and empirical studies have indicated that many individual characteristics of ice formed by processes of net basal adfreezing may be sensitive to the rate of propagation of the freezing front through the reservoir concerned. The effects of freezing rate on the stable-isotope chemistry and crystallography of ice, in addition to the disposition and character of included debris and gas are reported. Unidirectional freezing through a cylindrical reservoir containing various water-sediment mixtures has been conducted in the laboratory and the resulting cores analysed for debris and gas disposition and ice-crystal size and fabric. The data lend support to inferences drawn from studies concerned with specific ice properties and an idealized suite of characteristics is developed which may be diagnostic of basal ice formed by net adfreezing.

### INTRODUCTION

Basal ice forms and deforms at the bed of a glacier, an environment characterized by relatively high simple shear strain rates and complex fluctuations in ice pressure and temperature, often around the pressure-melting point. Thus, included debris (Weertman, 1968; Boulton, 1974), gas (Herron and Langway, 1979), crystal size and fabric (e.g. Kamb, 1972) and the solute content of the ice itself (Souchez and others, 1973) can all vary in response to conditions operative subsequent to ice accretion. However, the initial character of the ice, which is more or less affected by such changes, may itself provide invaluable information relating to the processes responsible for its formation.

Two dominant mechanisms have been advanced to explain the formation of relatively distinctive basal ice facies from the refreezing of water at the glacier bed. Current theories favour the process of "Weertman regelation" (Weertman, 1964) both for the formation of laminated ice facies, often identified in both temperate and sub-polar glaciers (Kamb and LaChapelle, 1964; Boulton, 1970) and of dispersed or "clotted" ice, more commonly reported in sub-polar glaciers only (Lawson, 1979; Sugden and others, 1987a; Souchez and others, 1988a). This mechanism of formation, involving the incremental, closed-system refreezing of thin layers of locally generated meltwater on the lee side of small bedrock bumps, is supported by detailed isotopic evidence (Lemmens and others, 1983; Sharp and others, 1990), ice chemistry (Hallet and others, 1978), debris-size analysis (Sugden and others, 1987a) and larger-scale facies relations (Sugden and others, 1987a). The second mechanism of ice formation is that of "net basal adfreezing" which involves the migration of the freezing front into saturated subglacial sediments (Weertman, 1961) or through water

trapped above a rock bed (e.g. Tison and Lorrain, 1987). Field evidence in support of such a mechanism of formation is somewhat disparate and relies largely on reports of intact sedimentary structures observed within elevated debris bands (Boulton, 1970; Harris and Bothamly, 1984) and facies relations, where stratified ice (consisting of alternating layers of debris-rich ice and clear ice, each some centimetres to tens of centimetres thick) often underlies dispersed ice, thereby indicating formation down-glacier, possibly in a marginal zone of ephemeral freezing conditions at the bed.

While several basal ice facies have been identified in the field, only the two basic mechanisms outlined above have been advanced to explain their formation and detailed relationships are not clear. For example, while most basal ice is devoid of bubbles owing to rejection during refreezing, Kamb and LaChapelle (1964) observed bubble planes within the regelation layer at Blue Glacier, Washington, and, indeed, took them to be diagnostic of the regelation process. More generally, both clotted ice and laminated ice are considered to form by Weertman regelation while the physical character of stratified ice facies varies widely from glacier to glacier, and may itself include zones of laminated ice (e.g. Sugden and others, 1987b; Souchez and others, 1988a). Accordingly, a number of authors have advanced explanations for some of the variability encountered in the field. Boulton (1970) has pointed to the possible role of substrate material insofar as net basal adfreezing above a bedrock interface will result in the incorporation of less-concentrated debris than will adfreezing through saturated sediment. Souchez and others (1988a) cited the work of Boulton (1975) and pointed to the role of mixing and dispersion of debris-rich regelation ice in the basal zone during "streaming" around bedrock bumps. Knight (1987) cited the theoretical treatment of Lliboutry (1986) in advancing the

hypothesis that the silt within clotted ice may have been introduced along intergranular veins under a pressure gradient away from the interface during regelation.

Significantly, there has been a growing awareness that the character of ice formed during the process of unidirectional adfreezing may be influenced to a large extent by the freezing rate, manifested as the speed at which the freezing front migrates through the water or saturated sediment reservoir concerned. Such an effect might go some way to accounting for hitherto unexplained variations between basal ice facies considered to have formed by the same process.

## THE INFLUENCE OF FREEZING RATE ON THE PHYSICAL PROPERTIES OF ADFROZEN ICE

### Included debris characteristics

Corte (1962) conducted a series of laboratory freezing experiments in which a horizontal, planar freezing front moved up through a cylindrical chamber. During the process, Corte seeded the advancing front with particles of various densities, sizes and shapes, and subsequently analysed the ice cores for evidence of preferential clast rejection in terms of the debris character and the freezing rates involved. He reported a crude inverse relationship between the freezing rate and the maximum size of particles forced ahead of the ice, and also that the shape of any particle, through its influence on the ratio of mass-to-contact area, played a role in the process such that "increasing the contact area of the particle while the size is constant causes the migration to increase" (Corte, 1962). Theory and modelling of the forces which result in individual particle rejection at the freezing interface have validated these observations. For example, Wilcox (1980) has equated the hydrodynamic force tending to push a spherical particle into an advancing freezing front with the disjoining pressure of the liquid film which exists between the ice and that particle. The author concluded that, for a particle being lifted against gravity, the critical freezing rate above which the particle will be entrapped varies inversely with the radius of the particle squared or cubed, depending on its size. Similar conclusions have been reached by Uhlmann and others (1964) from a series of experiments where particulate suspensions were frozen between two slides. Above a minimum size of c.15  $\mu\text{m}$ , a critical velocity for entrapment was identified as being inversely proportional to the diameter of the particle squared.

### Stable-isotope chemistry

More recently, Souchez and others (1987, 1988b) have dealt with the control exerted by freezing rate on the isotopic composition of ice. These authors pointed out that equilibrium fractionation represents only one extreme of a range of situations and that, in reality, the preferential incorporation of heavy isotopes into the ice ( $^{18}\text{O}$  and  $\text{D}^{[2}\text{H}]$ ) at the interface is controlled by molecular diffusion across a thin "boundary layer", the thickness of which reflects the amount of mixing in the reservoir. Thus, in general, the faster the freezing rate the further the

preferential heavy-isotope incorporation from that described by the equilibrium-fractionation coefficient, corresponding to a Rayleigh-type distribution in the ice. In the experiments carried out by Arnason (1969), in order to determine empirically the fractionation coefficient for deuterium as water froze to ice, the author identified a rate of 2  $\text{mm h}^{-1}$  as being the threshold above which equilibrium fractionation did not occur. While this figure is specific to the particular apparatus used, quantitative assessment of the effect has come from Souchez and others (1987), who used a box-diffusion model to analyse the migration of isotopes through the boundary layer. These authors found that each combination of boundary-layer thickness and freezing rate resulted in a unique isotopic distribution within the refrozen ice. Support for the model came from the analysis of lake-ice samples where theoretically determined freezing rates were in good agreement with those derived from known temperature fluctuations during the period of ice formation. Similarly, satisfactory results have been obtained for sea-ice growth rates in a core from Breid Bay, Antarctica (Souchez and others, 1988b).

### Gas nucleation

The thermodynamics of gas precipitation from solution and consequent debris entrapment in freezing liquids may also be intimately associated with the rate of advance of the freezing front. Controlled laboratory experiments carried out by Rowell and Dillon (1972) demonstrated that, where 50 ml cylinders of various electrolytes containing clay suspensions were frozen from the base at c.10  $\text{mm h}^{-1}$  and from the sides at c.1  $\text{mm h}^{-1}$ , gas bubbles in the resulting frozen cores were observed to have been preferentially precipitated in thin horizontal bands separated by relatively clear ice containing occasional vertical bubble lineations, parallel to the direction of freezing. Additionally, it was observed that the ice which had experienced slow freezing around the outside of the samples was completely free of bubbles. The formation of this bubble-free ice is consistent with processes of efficient gas rejection at a slowly advancing freezing front as described by Hallet (1976), yet the horizontal layering through the rest of the sample requires further explanation. The authors stated that, as the solution freezes and both air and electrolyte are displaced into the liquid ahead of the interface, the concentrations of these increase in the liquid until saturation or supersaturation is reached and air nucleates to form gas bubbles. At this point, the sudden reduction in the concentration of dissolved gas at the interface causes the freezing point of the liquid around the bubbles to rise and results in the rapid freezing of a layer of liquid, with insufficient time for the bubbles to migrate away from the front. Support for this theory came from observations that fewer bubbles, in layers further apart, were observed in ice formed from freshly boiled water than in ice formed from distilled water. Corte (1961) froze 5 mm thick layers of water between glass slides and reported the concentration of trapped air bubbles (radius  $R$ ) to be proportional to  $R^{1.7}$ , while a threshold existed at a freezing rate of c.17  $\mu\text{m s}^{-1}$  (61  $\text{mm h}^{-1}$ ) with bubbles forming as cylinders parallel to the growth direction below this, while bubbles were egg-shaped (with their

narrow ends aligned towards the interface) at rates faster than this. In the freezing experiments of Bari and Hallet (1974), a similar threshold was identified, along with another at  $2\text{--}4\ \mu\text{m s}^{-1}$  ( $7.2\text{--}14.4\ \text{mm h}^{-1}$ ) below which no bubbles formed at all. However, any quantitative analysis of bubble nucleation is problematic as the initial gas and debris content of the water must also be taken into account. These authors also observed a crude bubble layering parallel to the freezing front similar to that reported by Rowell and Dillon (1972), which they explained in terms of non-linear variations in the relationship between gas saturation at the interface and phases of nucleation.

Rowell and Dillon (1972) made the additional observation that the formation of bands of air bubbles parallel to the freezing front also played a central role in the incorporation of clay-rich layers in those cases where solutions containing suspended, dispersed clays were frozen. Similar to both the electrolyte and the dissolved gas, and in accordance with the work of Corte (1962) and Wilcox (1980) cited above, dispersed clay particles were observed to migrate in front of the advancing freezing front, but only until gas precipitation occurred. At this point, debris was trapped within the bubbles and thereby incorporated into the ice. The hypothesized enhanced freezing rate through these bubbly zones would also be conducive to debris incorporation, particularly if, during freezing in the presence of high electrolyte concentrations, some of the clays had formed into small aggregates, as was observed by the authors upon thawing the cores.

In some more recent work, Clayton and others (1990) have documented debris disposition in ice formed from lateral freezing through a cylinder containing an aqueous suspension of clays. With a homogeneous distribution at the onset of freezing, the authors reported not only that particles had been pushed towards the centre of the container (resulting in c. 2 cm of clear ice around the outside of the core) but also that segregation by size had occurred within the interior zone such that finer particles were moved more effectively by the freezing front (according with the experimental results of Corte and the theoretical treatment by Wilcox outlined above). Significantly, such preferential exclusion resulted in debris banding where "the concentric rings approximately half-way into the cross-section are comprised mostly of larger particles, while smaller, less distinct particles cause the 'turbid' appearance at the centre of the cross section". This sorting process resulted in corresponding variations in debris concentration through the core (personal communication from J. R. Clayton).

### Ice crystallography

Ice crystallography (grain-size, shape and fabric) may also be diagnostic of unidirectional adfreezing. As in the solidification of metamorphic rocks, grain-size is inversely related to the rate of freezing while crystal shape and fabric may be strongly controlled by the direction of the migration of the freezing front through the liquid. Shumskiy (1964) analysed the process of geometric selection during orthotropic crystallization whereby more favourably oriented grains capture less effective competitors, usually within 50–100 times the mean diameter of the

crystals in the initial layer. During this process the orientations of the main crystal axes can align themselves either normal to the surface of freezing or parallel to it (Shumskiy, 1964) while more rapid cooling results in stronger fabrics (more uniform orientations) through reducing the thickness of the supercooled layer immediately adjacent to the ice crystals. Tison and Lorrain (1987) have analysed the crystallography of ice from a cavity beneath Glacier de Tsanfleuron, Switzerland, at three stages as it progressed from an undeformed floor-ice coating to full incorporation within the basal layer of the glacier. In horizontal section, the initial fabric of the floor-ice layer was largely equatorial with a certain number of randomly orientated grains. In addition, crystal shape was anhedral perpendicular to the direction of freezing and grains were elongated in the direction of freezing. As this ice was picked up by the glacier and incorporated into the basal layer, the fabric evolved progressively to a bimodal form under the influence of the dominant pure shear-stress field.

Strong evidence therefore exists not only to support the argument that ice formed by unidirectional net adfreezing should be identifiable in terms of its physical characteristics but also that the rate of freezing involved may exert a significant influence over the detail of those characteristics, particularly the debris, gas and isotopic content of the ice. In certain cases, the distribution of gas bubbles and fine debris in the ice, and the freezing rate may be interdependent and linked in a complex manner.

A series of controlled laboratory freezing experiments has been carried out in order to investigate such relationships further.

### EXPERIMENTAL APPARATUS AND PROCEDURE

A cylindrical, "plexiglass" freezing chamber was designed such that ice cores could be frozen with a horizontal, planar freezing front moving either up or down through the reservoir (Fig. 1). The heat sink was supplied by circulating alcohol, the temperature of which was controlled by a regulated cooling element. In experiments where ice was frozen down from the top, the escape of

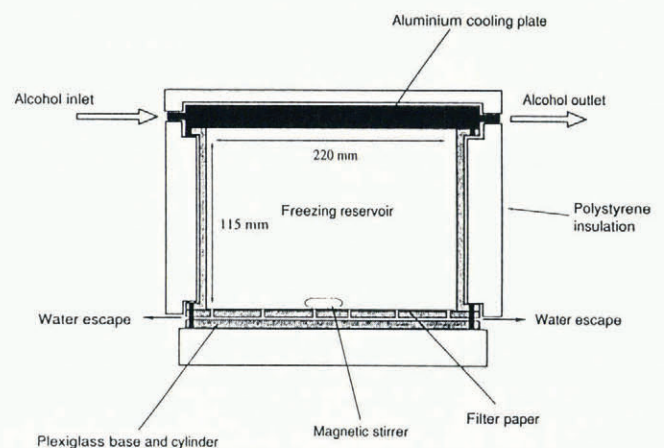


Fig. 1. The freezing apparatus as utilized for freezing downward. The aluminium cooling plate replaces the "plexiglass" base plate for upwards freezing.

pressurized water was facilitated through holes drilled into the base. The apparatus was insulated such that the propagation of the freezing front through the reservoir (and therefore the freezing rate) varied with  $T^{-1/2}$ , where  $T$  is time elapsed since the initiation of freezing. All cores were analysed and sampled in a cold room at an ambient temperature of c.  $-14^{\circ}\text{C}$ , cut with a mechanical band saw and thin sections reduced with a microtome.

Five experiments were conducted, each with different initial conditions in terms of certain parameters considered to influence basal ice formation in its natural setting. In addition to altering the rate of freezing, agitation of the reservoir was facilitated using a magnetic stirrer in order to observe the effects of turbulence at the basal interface. Both downward and upward freezing were induced and, although the former is more common, the latter is feasible and demonstrates better the processes operative through isolating the effects of gravity. Upward freezing has been hypothesized beneath Glacier de Tsijiore Nouve, Switzerland, by Souchez and Tison (1981), where the cationic chemistry of the ice led the authors to postulate freezing of meltwater within porous subglacial sediments owing to a drop in pressure there. Clear ice then formed above the impermeable frozen sediments. Similarly, Tison and Lorrain (1987) described the progressive upward freezing of meltwater during the formation of floor-ice coatings beneath Glacier de Tsanfleuron. In the present study, both the net concentration and size distribution of the debris were adjusted in order to mimic the freezing of either a saturated sediment or a meltwater suspension of variable turbidity. In upward-freezing experiments, debris was poured evenly into the reservoir as soon as a layer of ice was seen to have formed at the base and, while coarser fractions settled rapidly on to the interface, the finer fractions remained in suspension. All debris was stored

below  $0^{\circ}\text{C}$  in order to avoid melting at the interface as it settled. A summary of the experiments is given in Table 1 and the resulting cores were analysed for the following characteristics:

- (1) Ice crystallography: grain-size and  $c$ -axis orientation.
- (2) Debris disposition and character.
- (3) Distribution and form of included gas.

**RESULTS**

**Ice crystallography**

(a) *Crystal size*

Thin sections were cut both from three horizontal sections through both cores 1 and 2, and as a single vertical section through each and analysed in the cold room using a universal stage. Data presented in Table 2 demonstrate a strong tendency for the ice crystals to grow in size parallel to the direction of the migration of the freezing front such that, in experiment 1 where freezing was downwards and the suspension stirred, the mean grain diameter increases continuously from 3.5 mm at a depth of 15–15.1 mm at approximately 85 mm from the top of the core. This represents the product of two complementary effects: first, the tendency for ice crystals to compete and “capture” or die out as the front propagates, and secondly, a tendency towards the growth of larger individual crystals at slower rates of formation.

Grain-size, however, is not only the product of the freezing rate and grain capture but may also be influenced by the debris content of the ice concerned (e.g. Baker, 1978). During freezing, ice-crystal growth is inhibited by the presence of debris such that particulate concentration

Table 1. Experimental parameters

Experiment No.	Direction	Stirred	Freezing rate $\text{mm h}^{-1}$	Debris grain-size classes					
				Diamict	< 63 $\mu\text{m}$	64–125 $\mu\text{m}$	126–250 $\mu\text{m}$	251–500 $\mu\text{m}$	501–1000 $\mu\text{m}$
1	Down	Y	$0.12 T^{-0.5}$	240 g	360 g				
2	Down	N	$0.18 T^{-0.5}$	240 g	360 g				
3	Up	N	$0.09 T^{-0.5}$	1125 g	125 g	250 g	250 g	250 g	
*				50 g	50 g	50 g	50 g	50 g	
4	Up	N	$0.98 T^{-0.5}$	x	20 g	20 g	20 g	20 g	20 g
5	Up	N	$4.55 T^{-0.5}$		20 g	20 g	20 g	20 g	20 g
†					20 g	20 g	20 g	20 g	20 g
‡					20 g	20 g	20 g	20 g	20 g

\* Debris added to freezing front at  $H = 50$  mm.

† Debris added to freezing front at  $H = 20$  mm.

‡ Debris added to freezing front at  $H = 42$  mm.

Table 2. Mean crystal diameter by thin section ("a" and "b" are the longest and shortest axes, respectively)

Experiment	Section	a-axis mm	b-axis mm	(a + b)/2 mm	Freezing rate mm h <sup>-1</sup>
1	H15	4.2	2.8	3.5	11.52
	H60	9.9	7.2	8.5	2.88
	H85	17.9	12.3	15.1	1.98
	Vertical	25.9	4.8	15.3	—
2	H18	2.9	1.4	2.2	20.42
	H45	2.6	1.5	2.3	8.40
	H85	11.0	6.6	8.8	4.45
	Vertical	24.5	4.1	14.3	—

\* H denotes depth below upper surface.

and grain-size are inversely related. This effect was borne out in all experiments, where it was found that the crystal size was very sensitive to the concentration of fine debris. Ice-crystal size in the field will additionally reflect the effects of strain rate, ice temperature and time since formation (through enhancing recrystallization), though these factors can usually be regarded as "constant" at a sufficiently local scale.

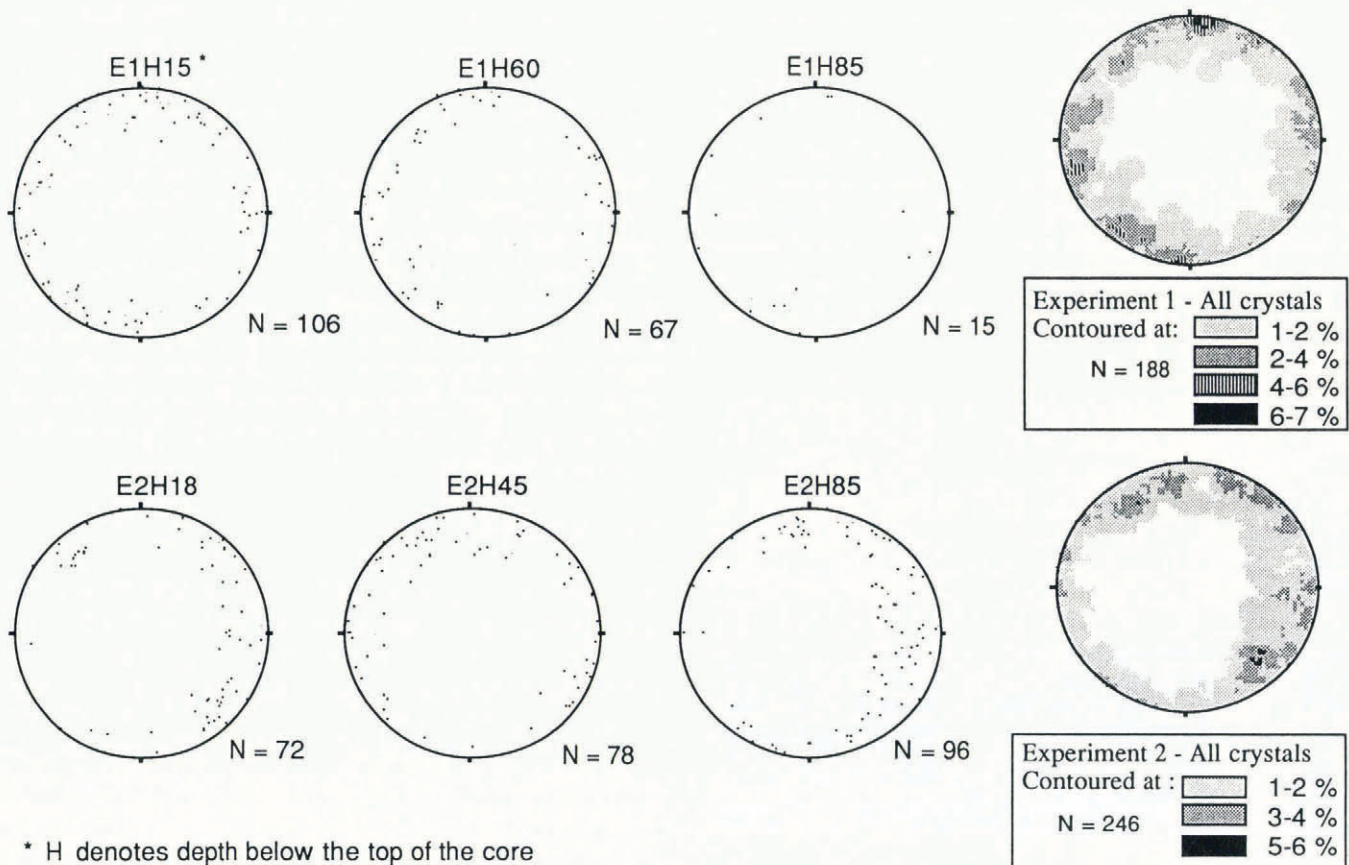
### (b) Crystal fabric

c-axis orientations were measured on each of the horizontal sections through cores 1 and 2, and hemispheric projections of the data are presented in Figure 2. Optic axes are aligned strongly in sub-horizontal positions, broadly parallel to the freezing front and perpendicular to the direction of its migration. This strong monoclinic distribution is in accordance with the work of Shumskiy (1964) and Tison and Lorrain (1987). The strikes of the crystal axes appear to be randomly distributed, as might be expected given the lack of any lateral component of freezing during grain formation. As a result of the highly variable sample numbers concerned, no relation can be determined between the freezing rate and the fabric strength.

### Sedimentology

#### (a) Debris disposition

In both experiments 1 and 2, where particle grain-size was less than 125 µm and exclusion at the interface was assisted by gravitational effects, the major part of the debris was rejected at the freezing front throughout the formation of the cores. In core 1, which was stirred, a very small amount of debris was incorporated both at the beginning of the experiment, when the freezing rate was high, and at the end when the debris concentration had risen such that clast-to-clast contacts may have prevented efficient migration away from the freezing front. Debris concentrations in six bands down the core are given in Table 3. Throughout the core, a small amount of fine debris was present on the walls of gas bubbles as a result of



\* H denotes depth below the top of the core

Fig. 2. Ice-crystal fabrics from cores 1 and 2 plotted on a Schmidt (equal area) net. H is the depth below the upper surface.

Table 3. Included debris concentration as measured in six bands down core 1

Thickness from top of core mm	Debris concentration g l <sup>-1</sup>
0–24	1.45
25–38	0.04
39–60	0.06
61–81	0.11
82–99	6.45
100–110	2024.21

incorporation at the interface at those locations where bubbles were engulfed by the advancing ice front. In situations where bubbles were not forming, the fines at the interface were pushed ahead of the advancing ice front. In experiments 3 and 5, where the propagation of the freezing front was upwards and debris up to 1 mm in diameter was supplied to the interface during the experiments, the freezing front passed through the debris but pushed a certain amount of the finer fraction ahead of it, lifting it out from the seeded band into the ice above (Fig. 3). In experiment 4, a saturated diamict from Glacier de Tsijiore Nouve, Switzerland, was frozen through from the base. As the freezing front migrated through the top of the diamict, it carried fine particles with it which were subsequently frozen into the ice above the debris (Fig. 4).

The debris carried out from the frozen bands in experiments 3 and 5 is clearly visible in cross-section (Fig. 3) and is not deposited evenly in the clearer ice above but as crude, low-concentration layers each up to 10 mm thick. These are created in the absence of associated bubble banding and may form as a result of the crossing of an internal threshold involving the gradual build-up of debris at the interface until the overburden resistance to the disjoining pressure is sufficient to prevent the rejection of the debris in contact with the ice. At this

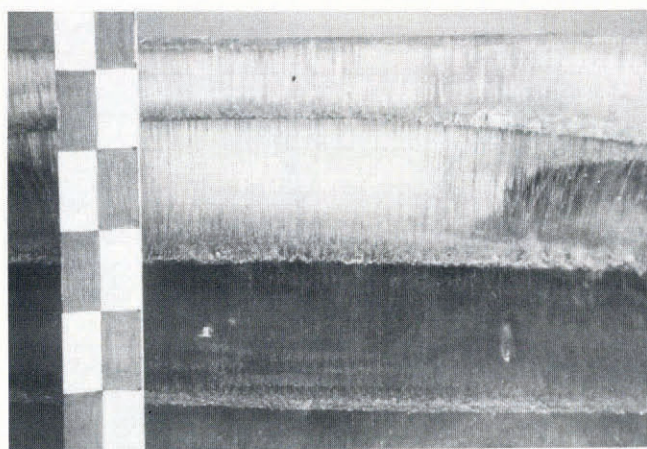


Fig. 3. Vertical section through core 5 demonstrating debris translocation from the seeded bands into crude layers in the overlying clearer ice.



Fig. 4. Fine debris elevated from a diamict from Glacier de Tsijiore Nouve (Switzerland) and frozen into the ice above. The contrast between the grain-size in this elevated band and the parent debris is highlighted in Figure 5a.

point, debris is incorporated into the growing ice, relieving the overburden pressure and once again facilitating the efficient rejection of all debris at the interface. The process will repeat until there is insufficient debris in the water to allow build-up above the interface to the extent required to overcome the forces of rejection. It appears, therefore, that debris banding may develop within the ice either in association with bubble nucleation or in its absence.

#### (b) Particle-size analysis

Where sufficient sample was recovered, debris weight was determined at intervals of 1  $\phi$ , by dry sieving from  $-5$  to  $5\phi$  and by laser granulometry from  $5$  to  $9\phi$ . The data from experiment 4 indicate objectively the ability of an advancing freezing front to push small particles ahead of it (Figs 4 and 5a). In this case, silt-sized particles were removed from the diamict while larger clasts remained relatively stable as the freezing front passed through the saturated debris. Similarly, grain-size distributions in three bands from core 5 (Fig. 5b) indicate a sorting effect, though it is less marked than in experiment 4. In this case, debris incorporated higher (later) in the core includes a greater proportion of fines and fewer larger clasts relative to the lowermost sampled debris band. This is taken as evidence for a small but continuous elevation of fines up through the core in association with the migration of the freezing front.

#### Gas distribution

In general, freezing rates were not fast enough to result in the production of the egg-shaped bubbles reported by Bari and Hallet (1974), yet clouds of fine bubbles and cylindrical bubbles, both occasionally in association with entrapped silt, were observed in the cores. The top 20 mm of core 1 was composed of clear ice, reflecting low gas concentrations in the initial water, even though the freezing rate was high and rejection therefore relatively ineffective. Beneath this layer, cylindrical bubbles formed, aligned perpendicular to the freezing front and thereafter, as the front migrated through the reservoir, these cylindrical bubbles could be observed extending from

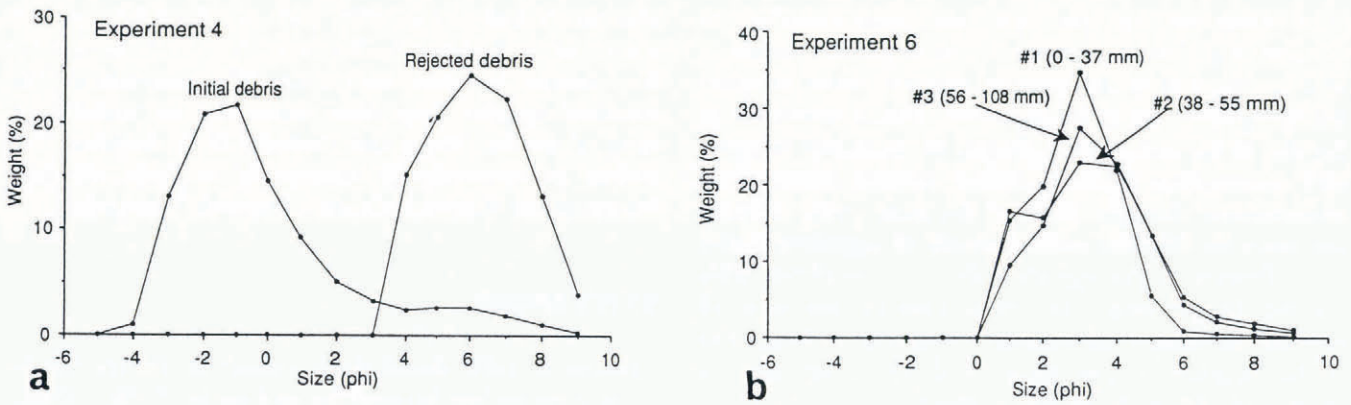


Fig. 5. Grain-size distributions of initial debris and elevated debris at various height intervals in core 4(a) and core 5(b).

Table 4. A summary of the likely effects of unidirectional planar adfreezing on the resulting ice

Physical characteristic	Freezing direction	Slower freezing rate	Faster freezing rate
<i>Crystallography</i>			
Size	—	Larger	Smaller
Shape	Anhedral perpendicular to freezing direction: elongated in direction of freezing	—	—
Fabric	Crystal orientation either parallel or perpendicular to the freezing direction	Weaker crystal fabric	Stronger crystal fabric
<i>Sedimentology</i>			
Particle distribution	Tendency towards layering parallel to the freezing front	More conspicuous layering due to more efficient rejection	Less-conspicuous layering due to less efficient rejection
Particle size	Possible sorting perpendicular to the freezing direction with larger grains preferentially incorporated in the ice between the layering	General absence of smaller particles incorporated in the ice between debris-rich layers	Smaller particles incorporated in ice between debris-rich layers
<i>Included gas</i>			
Bubble shape	Elongated in the direction of freezing. Possibly egg-shaped with narrow ends aligned towards the freezing interface	Tendency to form cylinders	Tendency to form discrete bubbles and bubble trains
Bubble distribution	Dispersed bubble trains and cylinders perpendicular to the freezing front. Discrete layering parallel to the freezing front	Lower bubble content and wider distribution of layers	Higher bubble content and less discrete layering
<i>Isotopic signature</i>			
	Characteristic isotopic profile perpendicular to freezing front	Fractionation coefficient approaches equilibrium resulting in Rayleigh-type distribution in the ice	Isotope distribution in the ice departs from that corresponding to equilibrium fractionation

the freezing front up into the ice. Any debris settling into the opening of these bubbles was subsequently incorporated on the wall of the growing cylinder while complete debris rejection was facilitated at the planar interface over the rest of the core. Such cylinders, occasionally widening and constricting to form linked bubble trains, were predominant through much of the core while, towards the base, the bubbles were observed to aggregate under the influence of the agitation due to the stirrer. This resulted in the production of a complex formation of bubbles of various dimensions including a large, flat bubble aligned in the plane of the freezing front of dimensions 40 mm × 30 mm × 5 mm.

A band of bubble cylinders, each elongated perpendicular to the freezing front, was observed to form in experiment 3 between heights of 5.3 and 5.6 cm at a freezing rate of under c. 1.9 mm h<sup>-1</sup> (0.5 μm s<sup>-1</sup>). The ice in this zone was a faint amber colour and closer inspection indicated again that fine particles had been incorporated on to the walls of these bubbles. While the formation of cylinders rather than bubble trains is consistent with low freezing rates, the actual observed rate here is significantly lower than the threshold identified by Bari and Hallett (1974) below which no bubbles formed in their experiments (2–4 μm s<sup>-1</sup>). This effect probably arises from the design of the freezing chambers utilized: in the present study, the upper surface of the freezing reservoir was partially sealed during upward-freezing experiments, with only a thin (c. 5 mm) layer of air present to accommodate expansion. In this case, the gas pressure was not atmospheric at the upper interface and diffusion away from the freezing front would have been correspondingly impeded, thereby inducing nucleation at lower freezing rates than in the open-system experiments of Bari and Hallett (1974).

## CONCLUSIONS

Basal ice formed by the process of net adfreezing may be distinguishable on account of the strong relationship between the mechanism of its initial formation and the physical characteristics of the ice. Work to date has dealt with the crystallographic and isotopic character of the ice and the character and distribution of the included gas and debris. Idealized relationships are outlined in Table 4, indicating that freezing-rate effects might explain much of the large variability in the character of stratified ice facies as reported in the literature. Rhythmic banding of debris included in basal ice might be partially explained in terms of cyclical expulsion during continuous net basal adfreezing, and may or may not be associated with similar phases of bubble nucleation and entrapment. However, such effects characterize the ice as initially formed and may, therefore, be altered or overprinted as a result of the subsequent history of that ice. Any interpretation of the character of basal ice as encountered in the field should therefore take into account both the initial character of that ice and its subsequent diagenesis.

## ACKNOWLEDGEMENTS

Gratitude is extended to all the staff at the Laboratoire de

Géomorphologie, Université Libre de Bruxelles, and in particular to Professor R. Souchez, Dr J.-L. Tison and Dr R. Lorrain for their assistance. The manuscript has benefited greatly from their comments in addition to those of Dr M. Sharp and Professor D. E. Sugden. The author is currently in receipt of a U.K. Natural Environment Research Council Research Studentship.

## REFERENCES

- Arnason, B. 1969. Equilibrium constant for the fractionation of deuterium between ice and water. *J. Phys. Chem.*, **73**(10), 3491–3494.
- Baker, R. W. 1978. The influence of ice-crystal size on creep. *J. Glaciol.*, **21**(85), 485–500.
- Bari, S. A. and J. Hallett. 1974. Nucleation and growth of bubbles at an ice–water interface. *J. Glaciol.*, **13**(69), 489–520.
- Boulton, G. S. 1970. On the origin and transport of englacial debris in Svalbard glaciers. *J. Glaciol.*, **9**(56), 213–229.
- Boulton, G. S. 1974. Processes and patterns of glacial erosion. In Coates D. R., ed. *Glacial geomorphology*. Binghamton, NY, State University of New York, 41–87.
- Boulton, G. S. 1975. Processes and patterns of subglacial sedimentation: a theoretical approach. In Wright, A. E. and F. Moseley, eds. *Ice ages: ancient and modern*. Liverpool, Steel House Press, 7–42.
- Clayton, J. R., Jr, E. Reimnitz, J. R. Payne and E. W. Kempema. 1990. Effects of advancing freeze fronts on distributions of fine-grained sediment particles in seawater- and freshwater-slush ice slurries. *J. Sediment. Petrol.*, **60**(1), 145–151.
- Corte, A. E. 1961. Air bubbles in ice. *Proc. Phys. Soc. London*, **77**(495), 757–768.
- Corte, A. E. 1962. Vertical migration of particles in front of a moving freezing plane. *J. Geophys. Res.*, **67**(3), 1085–1090.
- Hallett, B. 1976. Deposits formed by subglacial precipitation of CaCO<sub>3</sub>. *Geol. Soc. Am. Bull.*, **87**, 1003–1015.
- Hallett, B., R. D. Lorrain and R. Souchez. 1978. The composition of basal ice from a glacier sliding over limestones. *Geol. Soc. Am. Bull.*, **89**(2), 314–320.
- Harris, C. and K. Bothamley. 1984. Englacial deltaic sediments as evidence for basal freezing and marginal shearing, Leirbreen, southern Norway. *J. Glaciol.*, **30**(104), 30–34.
- Herron, S. and C. C. Langway, Jr. 1979. The debris-laden ice at the bottom of the Greenland ice sheet. *J. Glaciol.*, **23**(89), 193–207.
- Kamb, B. 1972. Experimental recrystallization of ice under stress. In Heard H. C., T. Y. Borg, N. L. Carter and C. B. Raleigh, eds. *Flow and fracture of rocks*. Washington, DC, American Geophysical Union, 211–241. (Geophysical Monograph **16**.)
- Kamb, B. and E. LaChapelle. 1964. Direct observation of the mechanism of glacier sliding over bedrock. *J. Glaciol.*, **5**(38), 159–172.
- Knight, P. G. 1987. Observations at the edge of the Greenland ice sheet: boundary condition implications for modellers. *International Association of Hydrological Sciences Publication 170* (Symposium at Vancouver 1987

- *The Physical Basis for Ice Sheet Modelling*), 359–366.
- Lawson, D. E. 1979. Sedimentological analysis of the western terminus region of the Matanuska Glacier, Alaska. *CRREL Rep.* 79-9.
- Lemmens, M., R. Lorrain and J. Haren. 1983. Isotopic composition of ice and subglacially precipitated calcite in an Alpine area. *Z. Gletscherkd. Glazialgeol.*, **18**(2), 1982, 151–159.
- Lliboutry, L. 1986. A discussion of Robin's "heat pump" effect by extending Nye's model for the sliding of a temperate glacier. *Eidg. Tech. Hochschule, Zürich. Versuchs-anst. Wasserbau, Hydrol. Glaziol. Mitt.* 90, 74–77.
- Rowell, D. L. and P. J. Dillon. 1972. Migration and aggregation of Na and Ca clays by the freezing of dispersed and flocculated suspensions. *J. Soil Sci.*, **23**(4), 442–447.
- Sharp, M., J.-L. Tison and G. Fierens. 1990. Geochemistry of subglacial calcites: implications for the hydrology of the basal water film. *Arct. Alp. Res.*, **22**(2), 141–152.
- Shumskiy, P. A. 1964. *Principles of structural glaciology*. New York, Dover Publications.
- Souchez, R. A. and J.-L. Tison. 1981. Basal freezing of squeezed water: its influence on glacier erosion. *Ann. Glaciol.*, **2**, 63–66.
- Souchez, R. A., R. D. Lorrain and M. M. Lemmens. 1973. Refreezing of interstitial water in a subglacial cavity of an Alpine glacier as indicated by the chemical composition of ice. *J. Glaciol.*, **12**(66), 453–459.
- Souchez, R., J.-L. Tison and J. Jouzel. 1987. Freezing rate determination by the isotopic composition of the ice. *Geophys. Res. Lett.*, **14**(6), 599–602.
- Souchez, R., R. Lorrain, J.-L. Tison and J. Jouzel. 1988a. Co-isotopic signature of two mechanisms of basal ice formation in Arctic outlet glaciers. *Ann. Glaciol.*, **10**, 163–166.
- Souchez, R., J.-L. Tison and J. Jouzel. 1988b. Deuterium concentration and growth rate of Antarctic first-year sea ice. *Geophys. Res. Lett.*, **15**(12), 1385–1388.
- Sugden, D. E. and 6 others. 1987a. Evidence for two zones of debris beneath the Greenland ice sheet. *Nature*, **328**(6127), 238–241.
- Sugden, D. E., C. M. Clapperton, J. C. Gemmell and P. G. Knight. 1987b. Stable isotopes and debris in basal glacier ice, South Georgia, Southern Ocean. *J. Glaciol.*, **33**(115), 324–329.
- Tison, J.-L. and R. D. Lorrain. 1987. A mechanism of basal ice-layer formation involving major ice-fabric changes. *J. Glaciol.*, **33**(113), 47–50.
- Uhlmann, D. R., B. Chalmers and K. A. Jackson. 1964. Interaction between a particle and a solid-liquid interface. *J. Appl. Phys.*, **35**(10), 2986–2993.
- Weertman, J. 1961. Mechanism for the formation of inner moraines found near the edge of cold ice caps and ice sheets. *J. Glaciol.*, **3**(30), 965–978.
- Weertman, J. 1964. The theory of glacier sliding. *J. Glaciol.*, **5**(39), 287–303.
- Weertman, J. 1968. Diffusion law for the dispersion of hard particles in an ice matrix that undergoes simple shear deformation. *J. Glaciol.*, **7**(50), 161–165.
- Wilcox, W. R. 1980. Force exerted on a single spherical particle by a freezing interface: theory. *J. Coll. Interface Sci.*, **77**(1), 213–218.

*The accuracy of references in the text and in this list is the responsibility of the author, to whom queries should be addressed.*

*MS received 7 November 1990*